

Notes

A New Class of Eight-Membered $\text{Sn}_2\text{P}_2\text{O}_4$ Heterocycles. Crystal Structure and Electrolytic Dissociation in Solution of *cyclo*- $[\text{R}_2\text{Sn}(\text{OPPh}_2\text{O})_2\text{SnR}_2](\text{O}_3\text{SCF}_3)_2$ ($\text{R} = \text{Me}, t\text{-Bu}$)

Jens Beckmann,* Dainis Dakternieks, Andrew Duthie, and Cassandra Mitchell
Centre for Chiral and Molecular Technologies, Deakin University, Geelong 3217, Australia

Received December 26, 2002

Summary: The syntheses of *cyclo*- $[\text{R}_2\text{Sn}(\text{OPPh}_2\text{O})_2\text{SnR}_2](\text{O}_3\text{SCF}_3)_2$ ($\text{R} = \text{Me}$ (**1**), $t\text{-Bu}$ (**2**)) by the consecutive reaction of R_2SnO ($\text{R} = \text{Me}, t\text{-Bu}$) with triflic acid and diphenylphosphinic acid are presented. In the solid state, **1** and **2** were investigated by ^{119}Sn MAS and ^{31}P MAS NMR spectroscopy as well as X-ray crystallography and appear to exist as ion pairs of *cyclo*- $[\text{R}_2\text{Sn}(\text{OPPh}_2\text{O})_2\text{SnR}_2]^{2+}$ dications and triflate anions. In solution, **1** and **2** are involved in extensive equilibria processes featuring cationic diorganotin(IV) species with Sn–O–P linkages, as evidenced by ^{119}Sn and ^{31}P NMR spectroscopy, electrospray mass spectrometry, and conductivity measurements.

Introduction

Organotin(IV) oxo clusters in general, and organotin(IV) phosphates, -phosphonates, -phosphinates, and related derivatives containing Sn–O–P linkages in particular, have attracted considerable attention in recent years owing to the intriguing diversity of their structures and association modes.¹ Triorganotin phosphinates, $\text{R}_3\text{SnO}_2\text{PR}'_2$ ($\text{R} = \text{alkyl}$; $\text{R}' = \text{alkyl}, \text{alkoxy}$), adopt either tetrameric,² hexameric,³ or polymeric structures in the solid state.⁴ Variable-temperature ^{31}P and ^{119}Sn NMR studies have demonstrated that tributyltin species $(\text{Bu}_3\text{SnO})_n\text{P}(\text{O})\text{Ph}_{3-n}$ ($n = 1-3$) are also autoassociated to varying degrees in solution.⁵ Monoorganotin compounds featuring Sn–O–P linkages are numerous and adopt cluster-type structures that have been classified as drums, prismanes, cubes, butterflies, crowns, etc.⁶ Most of these compounds are readily soluble in organic solvents and have been extensively investigated using ^{31}P and ^{119}Sn NMR spectroscopy.

By contrast, all reported diorganotin(IV) species hav-

ing Sn–O–P linkages appear to be polymeric. Many of these compounds comprise ill-defined amorphous materials that exhibit poor solubility in common organic solvents. Crystalline examples that were characterized by X-ray crystallography include $\text{R}_2\text{Sn}(\text{O}_2\text{PPh}_2)_2$ ($\text{R} = \text{Me}, \text{Et}$),⁷ $\text{R}_2\text{Sn}(\text{O}_2\text{PMe}_2)_2$ ($\text{R} = \text{Et}, \text{Ph}$),⁸ and $\text{Bu}_2\text{Sn}[\text{O}_2\text{P}(\text{OH})\text{Me}]_2$ ⁹ and contain eight-membered $\text{Sn}_2\text{P}_2\text{O}_4$ ring units incorporated into polymeric structures.

In the present work, we describe the preparation of *cyclo*- $[\text{R}_2\text{Sn}(\text{OPPh}_2\text{O})_2\text{SnR}_2](\text{O}_3\text{SCF}_3)_2$ ($\text{R} = \text{Me}$ (**1**), $t\text{-Bu}$ (**2**)) and provide evidence that these compounds exist as ion pairs of *cyclo*- $[\text{R}_2\text{Sn}(\text{OPPh}_2\text{O})_2\text{SnR}_2]^{2+}$ dications and triflate anions in the solid state. In solution, compounds **1** and **2** are involved in complex equilibria processes, which feature a number of cationic diorganotin(IV) species with Sn–O–P linkages.

Discussion

The reaction of polymeric dimethyltin oxide or trimeric di-*tert*-butyltin oxide with triflic acid in acetonitrile resulted in clear solutions containing solvated diorganotin hydroxide cations, $[\text{R}_2\text{Sn}(\text{OH})]^+$ ($\text{R} = \text{Me}, t\text{-Bu}$), as sole species.^{10,11} The subsequent reaction with diphenylphosphinic acid led to condensation and formation of crystalline *cyclo*- $[\text{R}_2\text{Sn}(\text{OPPh}_2\text{O})_2\text{SnR}_2](\text{O}_3\text{SCF}_3)_2$ ($\text{R} = \text{Me}$ (**1**), $t\text{-Bu}$ (**2**)) in high yields (eq 1).

The crystal structures of **1** and **2** comprise in the first approximation *cyclo*- $[\text{R}_2\text{Sn}(\text{OPPh}_2\text{O})_2\text{SnR}_2]^{2+}$ dications ($\text{R} = \text{Me}, t\text{-Bu}$) and loosely associated triflate anions (ion pairing) that fill the coordination sphere of the tin

(6) For a review see: (a) Holmes, R. R. *Acc. Chem. Res.* **1989**, *22*, 190. For more recent works see: (b) Chandrasekhar, V.; Baskar, V.; Steiner, A.; Zacchini, S. *Organometallics* **2002**, *21*, 4528. (c) Kumara Swamy, K. C.; Said, M. A.; Nagabrahmanandachari, S.; Poojary, D. M.; Clearfield, A. J. *Chem. Soc., Dalton Trans.* **1998**, 1645. (d) Nagabrahmanandachari, S.; Hemavathi, C.; Kumara Swamy, K. C.; Poojary, D. M.; Clearfield, A. *Main Group Met. Chem.* **1998**, *21*, 789.

(7) (a) Shihada, A. F.; Weller, F. Z. *Naturforsch.* **1996**, *B51*, 1111. (b) Shihada, A. F.; Weller, F. Z. *Anorg. Allg. Chem.* **2001**, *627*, 638.

(8) Shihada, A. F.; Weller, F. Z. *Naturforsch.* **1997**, *B52*, 587.

(9) Ribot, F.; Sanchez, C.; Biesemans, M.; Mercier, F. A. G.; Martins, J. C.; Gielen, M.; Willem, R. *Organometallics* **2001**, *20*, 2593.

(10) Upon removal of the solvent, dimeric diorganotin hydroxides $[\text{R}_2\text{Sn}(\text{OH})]_2(\text{O}_3\text{SCF}_3)_2$ or dimeric tetraorganodistannoxanes $[\text{R}_2(\text{F}_3\text{CSO}_3)\text{SnOSn}(\text{O}_3\text{SCF}_3)\text{R}_2]_2$ and $[\text{R}_2(\text{HO})\text{SnOSn}(\text{O}_3\text{SCF}_3)\text{R}_2]_2$ ($\text{R} = \text{alkyl}$) were isolated: (a) Sakamoto, K.; Ikeda, H.; Akashi, H.; Fukuyama, T.; Orita, A.; Otera, J. *Organometallics* **2000**, *19*, 3242. (b) Orita, A.; Xiang, J.; Sakamoto, K.; Otera, J. *J. Organomet. Chem.* **2001**, *624*, 287.

* Corresponding author. E-mail: beckmann@deakin.edu.au. Fax: ++61-3-5227-1040.

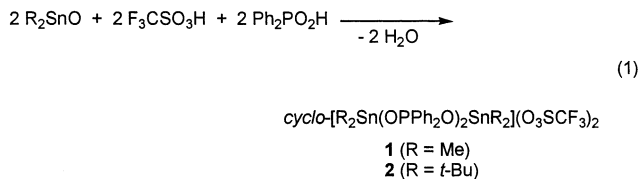
(1) For a recent review on organotin oxo clusters see: (a) Chandrasekhar, V.; Nagendran, S.; Baskar, V. *Coord. Chem. Rev.* **2002**, *235*, 1. For a review on SnOP species see: (b) Jain, V. K. *Coord. Chem. Rev.* **1994**, *135/136*, 809.

(2) Newton, M. G.; Haiduc, I.; King, R. B.; Silvestru, C. *J. Chem. Soc., Chem. Commun.* **1993**, 1229.

(3) (a) Molloy, K. C.; Nasser, F. A. K.; Barnes, C. L.; Van der Helm, D.; Zuckerman, J. J. *Inorg. Chem.* **1982**, *21*, 960. (b) Masters, J. G.; Nasser, F. A. K.; Hossain, M. B.; Hagen, A. P.; Van der Helm, D.; Zuckerman, J. J. *J. Organomet. Chem.* **1990**, *385*, 39.

(4) Weller, F.; Shihada, A. F. *J. Organomet. Chem.* **1987**, *322*, 185.

(5) Blunden, S. J.; Hill, R.; Gillies, D. G. *J. Organomet. Chem.* **1984**, *270*, 39.



atoms, as shown in Figures 1 and 2; selected bond parameters and crystal details are collected in Tables 1 and 2. Owing to the high Lewis acidity of the Me_2Sn moiety, two triflate anions are coordinated at each tin atom of **1** (4+2 coordination), whereas only one triflate anion adds to the geometry of the tin atoms in **2** (4+1 coordination). This arrangement necessitates that each triflate anion in **1** is involved in coordination of two adjacent tin atoms in the crystal lattice and, thus, gives rise to a two-dimensional coordination polymer that proceeds in the direction of the crystallographic *a*-axis (symmetry operation: $b = 1 + x, y, z$) (Figure 1). By contrast, the structure of **2** is essentially monomeric (Figure 2). The $\text{Sn}_2\text{P}_2\text{O}_4$ ring structure of **1** consists of two crystallographically independent P and Sn atoms, whereas that of **2** possesses an inversion center and consequently the P and Sn atoms are crystallographically related (symmetry operation $a = -x, -y, z$). The Sn atoms in **1** adopt strongly distorted octahedral geometries defined by C_2O_4 donor sets. The distortion is best documented in two sets of considerably different Sn– O_P and Sn– O_S bond lengths at 2.063(3)/2.093(3) and 2.434(4)/2.602(4) Å for Sn1 and at 2.066(3)/2.101(3) and 2.421(6)/2.607(4) Å for Sn2. The distortion is also revealed in the calculated bond orders¹² of 0.74/0.67 and 0.22/0.13 for Sn1 and of 0.73/0.65 and 0.23/0.13 for Sn2, respectively. Owing to the bulky *tert*-butyl groups, the two symmetry equivalent tin atoms in **2** adopt a strongly distorted trigonal bipyramidal geometry defined by a C_2O_3 donor set (geometrical goodness:¹³ $\Delta\Sigma(\theta) = 81.2^\circ$), in which two C atoms and one O_P atom occupy the equatorial positions, whereas the other O_P atom and the O_S atom are situated in the axial positions. This arrangement may explain the different Sn– O_P bond lengths at 2.045(3)/2.173(4) Å and show the apparently weaker coordination of the triflate anion defined by the Sn– O_S bond length of 2.302(5) Å (bond orders:¹² 0.78/0.52 and 0.34). The distinctively different Sn– O_P and Sn– O_S bond lengths provide evidence to suggest that **1** and **2** exist as ion pairs of $\text{cyclo-}[\text{R}_2\text{Sn}(\text{OPPh}_2\text{PO})_2\text{SnR}_2]^{2+}$ dications (R = Me, *t*-Bu) and triflate anions. The P–O bond lengths of **1** and **2** (average 1.511(4) Å) are almost equal within experimental error and are consistent with literature values reported for $\text{R}_2\text{Sn}(\text{O}_2\text{PPh}_2)_2$ (R = Me, Et),⁷ $\text{R}_2\text{Sn}(\text{O}_2\text{PMe}_2)_2$ (R = Et, Ph),⁸ and $\text{Bu}_2\text{Sn}[\text{O}_2\text{P}(\text{OH})\text{Me}]_2$.⁹ It is worth mentioning that the eight-membered $\text{Sn}_2\text{P}_2\text{O}_4$ heterocycles adopt in both compounds highly puckered ring conformations (puckering factor¹⁴ $a =$

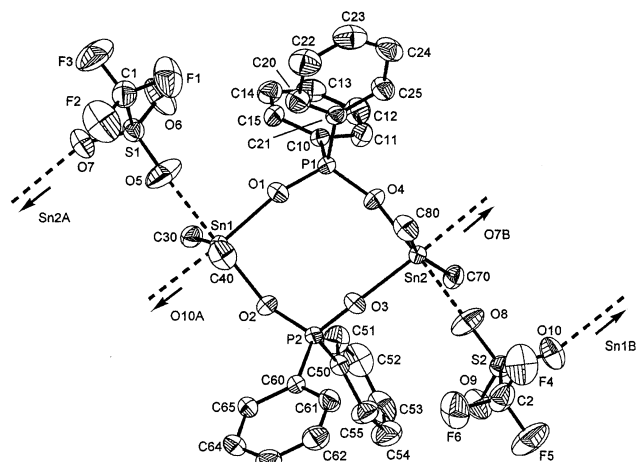


Figure 1. General view of **1** showing 30% probability displacement ellipsoids and the atom-numbering scheme (symmetry operation used to generate equivalent atoms: $b = 1 + x, y, z$).

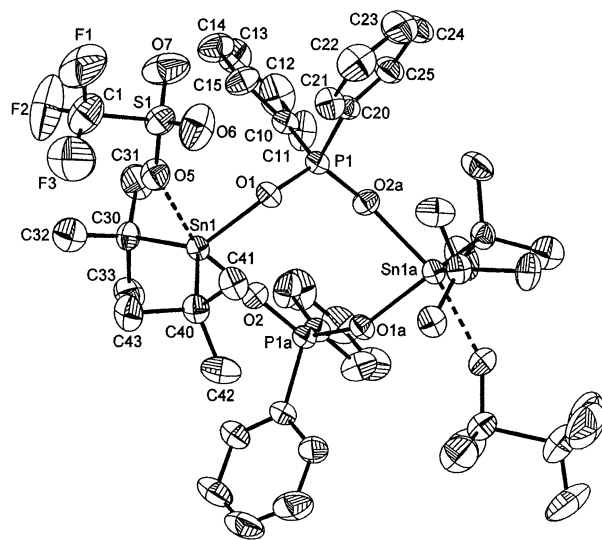


Figure 2. General view of **2** showing 30% probability displacement ellipsoids and the atom-numbering scheme (symmetry operation used to generate equivalent atoms: $a = -x, -y, z$).

0.940 for **1** and $a = 0.921$ for **2**). The ^{119}Sn MAS NMR spectrum of **1** shows a signal at $\delta -326.0$ ppm, which agrees well the 4+2 coordination found in the X-ray structure. However the spectrum failed to resolve the two crystallographically independent tin sites. The ^{119}Sn MAS NMR spectrum of **2** exhibits two signals at $\delta -321.1$ and -327.3 with approximately the same intensity, consistent with the 4+1 coordination established by X-ray diffraction. The observation of two very similar signals was tentatively attributed to the presence of a second polymorph present in the bulk material, which remained unaccounted for by X-ray crystallography. The ^{31}P MAS NMR spectra of **1** and **2** revealed two equally intense signals at $\delta 26.0$ and 21.5 and at $\delta 29.5$ and 27.3 , respectively. It is worth noting that no $^2J(^{31}\text{P}-\text{O}-^{117/119}\text{Sn})$ couplings were observed for **1** and **2** in the solid state.

Both compounds $\text{cyclo-}[\text{R}_2\text{Sn}(\text{OPPh}_2\text{O})_2\text{SnR}_2](\text{O}_3\text{SCF}_3)_2$ (R = Me (**1**), *t*-Bu (**2**)) are readily soluble in solvents such

(11) For the speciation of solvated dialkyltin dications, dialkyltin hydroxide cations, and related compounds in polar solvents see: (a) Tobias, R. S.; Ogrins, I.; Nevett, B. A. *Inorg. Chem.* **1962**, *1*, 638. (b) Tobias, R. S.; Yasuda, M. *Can. J. Chem.* **1964**, *42*, 781. (c) Tobias, R. S.; Farrer, H. N.; Hughes, M. B.; Nevett, B. A. *Inorg. Chem.* **1966**, *5*, 2052. (d) Arena, G.; Purrello, R.; Rizzarelli, E.; Gianguzza, A.; Pellerito, L. *J. Chem. Soc., Dalton Trans.* **1989**, 773. (e) Natsume, T.; Aizawa, S.; Hatano, K.; Funahashi, S. *J. Chem. Soc., Dalton Trans.* **1994**, 2749.

(12) Definition of bond order: $\log \text{BO} = -c(d - d_0)$; $c = 1.41$, $d_{\text{Sn-O}}(\text{Sn-O}) = 1.97$ Å: (a) Zickgraf, A.; Beuter, M.; Kolb, U.; Dräger, M.; Tozer, R.; Dakternieks, D.; Jurkschat, K. *Inorg. Chim. Acta* **1998**, *275-276*, 203. (b) Britton, D.; Duntiz, J. D. *J. Am. Chem. Soc.* **1981**, *103*, 2971.

(13) Kolb, U.; Beuter, M.; Dräger, M. *Inorg. Chem.* **1994**, *33*, 4522.

(14) Beckmann, J.; Jurkschat, K.; Schürmann, M.; Dakternieks, D.; Lim, A. E. K.; Lim, K. F. *Organometallics* **2001**, *20*, 5125.

Table 1. Selected Bond Lengths (Å) and Bond Angles (deg) for **1 and **2**^a**

	1 (X = 2, Y = 4)	2 (X = 1a, Y = 2a)
Sn(1)–O(1)	2.063(3)	2.045(3)
Sn(1)–O(2)	2.093(3)	2.173(4)
Sn(1)–O(5)	2.434(5)	2.302(5)
Sn(1)–O(10b)	2.602(4)	
Sn(1)–C(30)	2.090(5)	2.195(6)
Sn(1)–C(40)	2.097(7)	2.193(5)
Sn(2)–O(3)	2.066(3)	
Sn(2)–O(4)	2.101(3)	
Sn(2)–O(7b)	2.607(4)	
Sn(2)–O(8)	2.421(6)	
Sn(2)–C(70)	2.094(4)	
Sn(2)–C(80)	2.079(4)	
P(1)–O(1)	1.506(3)	1.518(4)
P(1)–O(Y)	1.513(3)	1.499(5)
P(1)–C(10)	1.785(5)	1.795(5)
P(1)–C(20)	1.783(4)	1.797(6)
P(2)–O(2)	1.517(4)	
P(2)–O(3)	1.515(3)	
P(2)–C(50)	1.789(4)	
P(2)–C(60)	1.786(4)	
O(1)–Sn(1)–O(2)	92.63(11)	83.43(13)
O(1)–Sn(1)–C(30)	97.39(15)	125.64(19)
O(1)–Sn(1)–C(40)	96.07(19)	106.68(20)
O(2)–Sn(1)–C(30)	91.40(15)	92.79(19)
O(2)–Sn(1)–C(40)	98.55(19)	101.83(18)
C(30)–Sn(1)–C(40)	162.85(21)	126.96(21)
O(3)–Sn(2)–O(4)	91.21(11)	
O(3)–Sn(2)–C(70)	101.68(15)	
O(3)–Sn(2)–C(80)	93.76(17)	
O(4)–Sn(2)–C(70)	90.16(15)	
O(4)–Sn(2)–C(80)	98.78(16)	
C(70)–Sn(2)–C(80)	162.01(18)	
O(1)–P(1)–O(Y)	115.56(18)	114.63(22)
O(1)–P(1)–C(10)	110.04(17)	109.23(23)
O(1)–P(1)–C(20)	106.80(18)	107.16(23)
O(Y)–P(1)–C(10)	106.19(16)	109.37(25)
O(Y)–P(1)–C(20)	109.24(18)	109.74(24)
C(10)–P(1)–C(20)	108.89(21)	106.38(26)
O(2)–P(2)–O(3)	114.49(18)	
O(2)–P(2)–C(50)	106.53(19)	
O(2)–P(2)–C(60)	109.84(16)	
O(3)–P(2)–C(50)	109.88(19)	
O(3)–P(2)–C(60)	106.70(16)	
C(50)–P(2)–C(60)	109.35(20)	
Sn(1)–O(1)–P(1)	162.71(19)	143.05(20)
Sn(1)–O(2)–P(X)	141.97(19)	156.46(27)
Sn(2)–O(3)–P(2)	151.88(19)	
Sn(2)–O(4)–P(1)	144.22(19)	

^a Symmetry operation used to generate equivalent atoms: $a = -x, -y, z$; $b = 1 + x, y, z$.

as CHCl_3 , THF, or MeCN. The solution ^{119}Sn and ^{31}P NMR spectra of **1** and **2** are complex (see Experimental Section). For both compounds the number and broadness of the signals and the lack of $^2J(^{119}\text{Sn}-\text{O}-^{13}\text{P})$ couplings for most of the signals are consistent with the existence of a number of equilibria in solution; however, no definitive assignments of the signals were made. Variable-temperature (-80 to 80 °C) ^{119}Sn and ^{31}P NMR studies revealed that the position of some signals is very temperature dependent; however no substantial decrease in line width of the broad signal was observed. Additional evidence for the existence of equilibria processes and for species that might be involved in these equilibria was obtained from electrospray mass spectrometry (ESMS). This technique was designed for the detection of (trace amounts of) charged species in solution, while neutral species remain unaccounted for. It is important to emphasize that ESMS involves no ionization source, so that neither ionization nor fragmentation occurs and that all detected ions are already preformed in solution.¹⁵ Thus, the ESMS spectrum

Table 2. Crystal Data and Structure Refinement for **1 and **2****

	1	2
formula	$\text{C}_{30}\text{H}_{32}\text{F}_6\text{O}_{10}\text{P}_2\text{S}_2\text{Sn}_2$	$\text{C}_{42}\text{H}_{56}\text{F}_6\text{O}_{10}\text{P}_2\text{S}_2\text{Sn}_2$
fw, g mol ⁻¹	1030.00	1198.31
cryst syst	triclinic	orthorhombic
cryst size, mm	$0.05 \times 0.15 \times 0.45$	$0.10 \times 0.12 \times 0.45$
space group	$P\bar{1}$	$P2_12_12$
<i>a</i> , Å	10.7613(6)	14.7503(9)
<i>b</i> , Å	12.5211(7)	17.5026(10)
<i>c</i> , Å	15.5313(8)	9.9932(6)
α , deg	75.631(1)	90
β , deg	81.230(1)	90
γ , deg	80.160(1)	90
<i>V</i> , Å ³	1984.1(2)	2579.9(3)
<i>Z</i>	2	2
ρ_{calcd} , Mg m ⁻³	1.724	1.543
<i>T</i> , K	293(2)	293(2)
μ , mm ⁻¹	1.522	1.179
<i>F</i> (000)	1016	1124
θ range, deg	1.36 to 27.53	1.81 to 27.52
index ranges	$-12 \leq h \leq 13$ $-15 \leq k \leq 16$ $-15 \leq l \leq 20$	$-19 \leq h \leq 19$ $-21 \leq k \leq 22$ $-8 \leq l \leq 12$
no. of reflns collcd	12 647	16 384
completeness to θ_{max}	95.5%	99.8%
no. of indep reflns/ R_{int}	8732	5866
no. of reflns obsd with $(I > 2\sigma(I))$	7256	4998
no. refined params	478	326
Goof (F^2)	1.073	0.998
$R_1(F)$ ($I > 2\sigma(I)$)	0.0381	0.0511
$wR_2(F^2)$ (all data)	0.1076	0.1333
$(\Delta/\sigma)_{\text{max}}$	0.0026	0.0040
largest diff peak/hole, e Å ⁻³	1.027/−0.661	1.273/−1.023

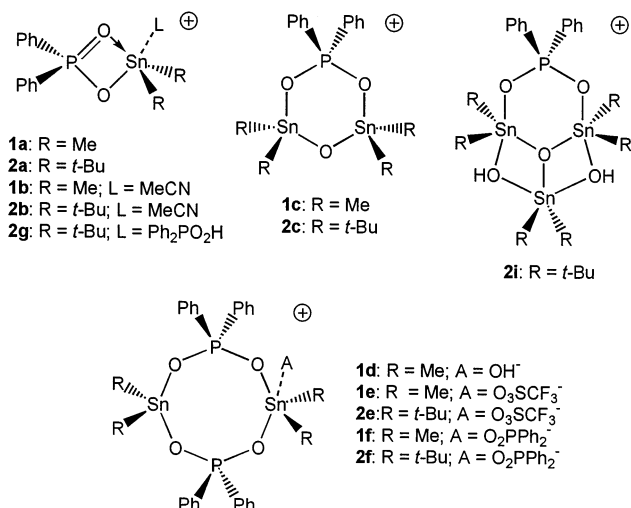
(positive mode, cone voltage 50 V) of **1** and **2** in MeCN revealed mass clusters with the expected isotope patterns at 367.0: $[\text{Me}_2\text{SnO}_2\text{PPh}_2]^+$ (**1a**), 408.0: $[\text{Me}_2\text{SnOPPh}_2\text{O}\cdot\text{MeCN}]^+$ (**1b**), 530.9: $[\text{Ph}_2\text{P}(\text{OSnMe}_2)_2\text{O}]^+$ (**1c**), 749.1: $[(\text{Me}_2\text{SnOPPh}_2\text{O})_2\cdot\text{OH}]^+$ (**1d**), 880.9: $[(\text{Me}_2\text{SnOPPh}_2\text{O})_2\cdot\text{O}_3\text{SCF}_3]^+$ (**1e**), 949.3: $[(\text{Me}_2\text{SnOPPh}_2\text{O})_2\cdot\text{O}_2\text{PPh}_2]^+$ (**1f**), and at 451.1: $[\text{t-Bu}_2\text{SnOPPh}_2\text{O}]^+$ (**2a**), 492.1: $[\text{t-Bu}_2\text{SnOPPh}_2\text{O}\cdot\text{MeCN}]^+$ (**2b**), 669.1: $[\text{t-Bu}_2\text{SnOPPh}_2\text{O}\cdot\text{Ph}_2\text{PO}_2\text{H}]^+$ (**2g**), 699.1: $[\text{Ph}_2\text{P}(\text{OSnt-Bu}_2)_2\text{O}]^+$ (**2c**), 887.4: $[\text{t-Bu}_2\text{SnOPPh}_2\text{O}\cdot(\text{Ph}_2\text{PO}_2\text{H})_2]^+$ (**2h**), 965.2: $[\text{Ph}_2\text{P}(\text{OSnt-Bu}_2)_2\text{O}\cdot\text{t-Bu}_2\text{Sn}(\text{OH})_2]^+$ (**2i**), 1049.1: $[(\text{t-Bu}_2\text{SnOPPh}_2\text{O})_2\cdot\text{O}_3\text{SCF}_3]^+$ (**2e**), 1115.4: $[(\text{t-Bu}_2\text{SnOPPh}_2\text{O})_2\cdot\text{O}_2\text{PPh}_2]^+$ (**2f**), respectively. Proposed structures of **1a–f** and **2a–i** are depicted in Chart 1. Interestingly, the *cyclo*- $[\text{t-Bu}_2\text{Sn}(\text{OPPh}_2\text{O})_2\text{Sn}(\text{t-Bu}_2)]^{2+}$ dication of **2** and the mass clusters of $[\text{Ph}_2\text{P}(\text{OSnt-Bu}_2)_2\text{O}]^+$ (**2c**) and $[\text{Ph}_2\text{P}(\text{OSnt-Bu}_2)_2\text{O}\cdot\text{t-Bu}_2\text{Sn}(\text{OH})_2]^+$ (**2i**) are isoelectronic with the recently reported stannasiloxanes *cyclo*- $[\text{t-Bu}_2\text{Sn}(\text{OSiPh}_2\text{O})_2\text{Sn}(\text{t-Bu}_2)]^{16}$ *cyclo*- $[\text{Ph}_2\text{Si}(\text{OSnt-Bu}_2)_2\text{O}]^{16,17}$ and $[\text{Ph}_2\text{Si}(\text{OSnt-Bu}_2)_2\text{O}\cdot\text{t-Bu}_2\text{Sn}(\text{OH})_2]^{17}$ respectively. While electrospray mass spectrometry allows no conclusions regarding the absolute concentration of the charged species in solution, conductivity measurements of **1** ($477 \mu\text{S cm}^{-1}$) and **2** ($563 \mu\text{S cm}^{-1}$) in MeCN ($c = 2.5 \text{ mmol L}^{-1}$) suggest that substantial concentrations of electro-

(15) For applications of electrospray mass spectrometry in organotin chemistry see: Dakternieks, D.; Lim, A. E. K.; Lim, K. F. *Phosphorus, Sulfur, Silicon* **1999**, 150–151, 339.

(16) Beckmann, J.; Mahieu, B.; Nigge, W.; Schollmeyer, D.; Schürmann, M.; Jurkschat, K. *Organometallics* **1998**, 17, 5697.

(17) Beckmann, J.; Jurkschat, K.; Mahieu, B.; Schürmann, M. *Main Group Met. Chem.* **1998**, 21, 113.

Chart 1



lytes are indeed present and that ionic species such **1a–f** and **2a–i** may play an important role for the equilibria processes in solution.

It was demonstrated recently that diorganotin(IV) species, such as [Bu₂Sn(OH)(H₂O)]₂(O₃SCF₃)₂¹⁸ or [Bu₂Sn(H₂O)₄](2,5-Me₂C₆H₃SO₃)₂,¹⁹ show high catalytic activities in acylation reactions, which was attributed to their ability to undergo electrolytic dissociations in polar solvents. The observation that **1** and **2** also form ions in solution may stimulate research toward their feasibility as catalysts for various organic reactions in the future.

Experimental Section

All solvents were distilled prior to use. Me₂SnO and *t*-Bu₂SnO were prepared according to literature procedures.²⁰ Ph₂PO₂H was purchased from Aldrich. The NMR spectra (concentration 50 mg/300 μL; 25 °C) were measured using a JEOL Eclipse Plus 400 spectrometer at 161.84 (³¹P) and 149.05 MHz (¹¹⁹Sn) and were referenced against aqueous H₃PO₄ (90%) and Me₄Sn. For the solid-state NMR spectra crystalline NH₄H₂PO₄ (δ 0.95) and *c*-Hex₄Sn (δ -97.35) were used as secondary references. The ¹¹⁹Sn MAS NMR spectra were obtained using cross polarization (contact time 5 ms, recycle delay 5–10 s). The ESMS spectra were obtained with a Platform II single quadrupole mass spectrometer (Micromass, Altrincham, UK) using a MeCN mobile phase. MeCN solutions (0.1 mM) were injected directly into the spectrometer via a Rheodyne injector equipped with a 50 μL loop. A Harvard 22 syringe pump delivered the solutions to the vaporization nozzle of the electrospray ion source at a flow rate of 10 μL min⁻¹. Nitrogen was used both as a drying gas and for nebulization with flow rates of approximately 200 and 20 mL min⁻¹, respectively. Pressure in the mass analyzer region was usually about 4 × 10⁻⁵ mbar. Typically 10 signal averaged spectra were collected. Microanalyses were carried out by CMAS, Belmont, Australia. The conductivity measurements were performed using a CDM80 conductivity meter equipped with a CDC104 conductivity cell (Radiometer Copenhagen, DK) at 25 °C.

Synthesis of *cyclo*-[R₂Sn(OPPh₂O)₂SnR₂](O₃SCF₃)₂ (R

(18) Sakamoto, K.; Hamada, Y.; Akashi, H.; Orita, A.; Otera, J. *Organometallics* **1999**, *18*, 3555.

(19) Chandrasekhar, V.; Boomishankar, R.; Singh, S.; Steiner, A.; Zacchini, S. *Organometallics* **2002**, *21*, 4575.

(20) (a) Rochow, E. G.; Seyferth, D. *J. Am. Chem. Soc.* **1953**, *75*, 2877. (b) Puff, H.; Schuh, W.; Sievers, R.; Wald, W.; Zimmer, R. *J. Organomet. Chem.* **1984**, *260*, 271.

= **Me (1)**, ***t*-Bu (2)**). To a suspension of the appropriate R₂SnO (1.65 g, 10.0 mmol for R = Me, 2.48 g, 10.0 mmol for R = *t*-Bu) in MeCN (20 mL), triflic acid (1.50 g, 10.0 mmol) was added via syringe. The mixture was stirred for 15 min to give a clear solution. Solid Ph₂PO₂H (2.18 g, 10.0 mmol) was added in one portion, and the mixture was heated for 30 min at 80 °C. In the case of R = Me, upon cooling, a colorless precipitate of Me₂Sn(O₂PPh₂)₂ (250 mg)⁷ formed, which was filtered off. The solvent was removed under reduced pressure, and the residue was recrystallized from hexane/CH₂Cl₂.

Compound 1: yield 4.38 g, 4.25 mmol, 85%; mp > 300 °C. Anal. Calcd for C₃₀H₃₂F₆O₁₀P₂S₂Sn₂ (1030.12): C, 34.98; H, 3.13. Found: C, 34.94; H, 2.94. ¹¹⁹Sn NMR δ: (CDCl₃) -318.0 (W_{1/2} = 400 Hz); (d₃-MeCN) -325.7 (W_{1/2} = 1500 Hz). ³¹P NMR δ: (CDCl₃) 39.2 (W_{1/2} = 10 Hz; integral 46%), 32.3 (W_{1/2} = 10 Hz; integral 46%), 13.8 (W_{1/2} = 50 Hz; integral 8%); (d₃-MeCN) 41.1 (W_{1/2} = 10 Hz; integral 2%), 37.8 (W_{1/2} = 50 Hz; integral 2%), and 28.4 (W_{1/2} = 500 Hz; integral 96%).

Compound 2: yield 5.45 g, 4.55 mmol, 91%; mp 186 °C (dec). Anal. Calcd for C₄₂H₅₆F₆O₁₀P₂S₂Sn₂ (1198.44): C, 42.09; H, 4.71. Found: C, 41.95; H, 4.65. ¹¹⁹Sn NMR δ: (CDCl₃) -261.0 (W_{1/2} = 800 Hz; integral 60%), -315.0 (W_{1/2} = 1000 Hz; integral 20%), -318.4 (triplet, ²J(¹¹⁹Sn-O-³¹P) = 240 Hz; integral 20%); (d₃-MeCN) -253.8 (doublet, ²J(¹¹⁹Sn-O-³¹P) = 150 Hz; integral 10%), -294.5 (W_{1/2} = 800 Hz; integral 10%), -307.3 (triplet, ²J(¹¹⁹Sn-O-³¹P) = 250 Hz; integral 80%). ³¹P NMR δ: (CDCl₃) 35.6 (²J(³¹P-O-^{119/117}Sn) = 150 Hz; integral 30%), 33.0 (W_{1/2} = 300 Hz; integral 55%), 28.4 (²J(³¹P-O-^{119/117}Sn) = 230 Hz; integral 15%), 35.1 (W_{1/2} = 50 Hz; integral 5%), 33.8 (W_{1/2} = 150 Hz; integral 45%), and 28.9 (²J(³¹P-O-^{119/117}Sn) = 245 Hz; integral 50%).

X-ray Crystallography. Intensity data for **1** and **2** were collected on a Bruker SMART Apex CCD diffractometer fitted with Mo Kα radiation (graphite crystal monochromator, *l* = 0.71073 Å) to θ_{max} via ω scans. Data were reduced and corrected for absorption using the programs SAINT and SADABS.²¹ The structure was solved by direct methods and difference Fourier synthesis using SHELX-97 implemented in the program WinGX 2002.²² Full-matrix least-squares refinement on *F*², using all data, was carried out with anisotropic displacement parameters applied to all non-hydrogen atoms. Hydrogen atoms were included in geometrically calculated positions using a riding model and were refined isotropically. Disorder was resolved for both *tert*-butyl groups so that the C31, C32, C33, and C42 methyl groups were refined over two sites with occupancy ratios of 50:50. For these carbon atoms no hydrogen atoms were included in the refinement. The absolute configuration of **2** was determined by a refinement of the Flack parameter: 0.05(3).²³

Crystallographic data (excluding structure factors) for the structural analyses have been deposited with the Cambridge Crystallographic Data Centre, CCDC nos. 208263 for **1** and 208264 for **2**. Copies of this information may be obtained free of charge from The Director, CCDC, 12 Union Road, Cambridge CB2 1EZ, UK (fax: +44-1223-336033; e-mail: deposit@ccdc.cam.ac.uk or <http://www.ccdc.cam.ac.uk>).

Acknowledgment. The Australian Research Council (ARC) is thanked for financial support. Dr. Jonathan White (Melbourne University) is gratefully acknowledged for the X-ray crystallography data collection.

Supporting Information Available: Tables of all coordinates, anisotropic displacement parameters, and geometric data for compounds **1** and **2**. This material is available free of charge via the Internet at <http://pubs.acs.org>.

OM021042U

(21) SMART, SAINT, and SADABS; Siemens Analytical X-ray Instruments Inc.: Madison, WI, 1999.

(22) Farrugia, L. J. *J. Appl. Crystallogr.* **1997**, *20*, 565.

(23) Flack, H. D. *Acta Crystallogr.* **1983**, *A39*, 876.